Multi-Neuromodulator Measurements across Fronto-Striatal Network Areas of the Behaving Macaque using Solid-Phase Microextraction

Seyed-Alireza Hassani[1,2,†] , Sofia Lendor[3,†] , Ezel Boyaci[3], Janusz Pawliszyn[3,‡,*] and Thilo Womelsdorf[1,2,‡,*]

1 Department of Psychology, Vanderbilt University, PMB 407817, 2301 Vanderbilt Place, Nashville TN 37240, USA
2 Department of Biology, Centre for Vision Research, York University, Toronto, Ontario M6J 1P3, Canada
3 Department of Chemistry, University of Waterloo, 200 University Avenue West, Waterloo, Ontario N2L 3G1, Canada

* Corresponding author 1: Tel. 519-888-4641, Fax. 519-746-0435, E-mail: janusz@uwaterloo.ca
* Corresponding author 2: Tel. 615-322-0070, E-mail: thilo.womelsdorf@vanderbilt.edu
† ‡ These authors contributed equally

Short title: Reliable in-vivo sensing of multiple neurotransmitters using SPME

Keywords: Glutamate; Dopamine; Acetylcholine; Excitation-inhibition balance; Basal Ganglia; Prefrontal Cortex

Number of figures: 2
Number of supplementary material: 4
supplementary methods, supplementary discussion, figures (2), tables (1)

Abstract

Different neuromodulators rarely act independent from each other to modify neural processes. To understand this interdependence in local circuits during different brain states, it is necessary to reliably extract local concentrations of multiple neuromodulators in vivo. Here we describe results using solid phase microextraction (SPME), a method providing sensitive, multi-neuromodulator measurements. Reliable measurements of glutamate, dopamine, acetylcholine and choline were made simultaneously within frontal cortex and striatum of two macaque monkeys during goal-directed behavior. We find glutamate concentrations several orders of magnitude higher than acetylcholine and dopamine in all brain regions. Dopamine was reliably detected in the striatum at tenfold higher concentrations than acetylcholine. Acetylcholine and choline concentrations were detected with high consistency across brain areas, within and between monkeys. These findings illustrate that SPME microprobes provide a versatile novel tool to characterize multiple neuromodulators across different brain areas in vivo to understand the interdependence and co-variation of neuromodulators during goal directed behavior.

Introduction

Extracellular concentrations of neuromodulators influence firing regimes, input-output relationships and neural interactions in local circuits and long-range brain networks [1,2], and are dysregulated in virtually all psychiatric disorders [3,4]. Accumulating evidence suggests that these fundamental roles of neuromodulators for circuit functioning are unlikely realized by single neuromodulators operating in isolation. Rather, neuromodulatory systems are heavily intertwined [4–6], and operate simultaneously on individual cells and circuits [2,7–9]. In each circuit, local

49 mechanisms exert control over the release of neuromodulators from terminals of brainstem-
50 originating projection neurons. This local control proceeds through activation of pre-synaptic
51 glutamatergic receptors such as AMPAR and NMDAR [10–12]. These insights suggest that an
52 understanding of the contribution of neuromodulators to circuit functioning requires measuring,
53 simultaneously, multiple neuromodulators in conjunction with ongoing glutamatergic
54 neurotransmitter concentrations and action. Consistent with this conclusion single
55 neuromodulator theories often fail to account for all observable symptoms in psychiatric diseases
56 [13–15].

57 Despite the accumulating evidence for the interdependence of neuromodulator actions,
58 few methods exist for their simultaneous measurement in vivo and across multiple brain areas
59 (**Table S1**). Most of these existing neurochemical sensing methods have a high barrier to entry
60 by requiring specialized equipment and trained experts preventing data collection by scientists
61 who are otherwise interested in the role of endogenous and exogenous neuroactive chemicals in
62 cognition and psychiatric disorders. Electrochemical methods such as fast scan cyclic
63 voltammetry (FSCV) and amperometry have sub-second temporal resolution, but are limited to
64 the measurement of a few compounds [16,17] and are not robust for in vivo application in
65 nonhuman primates [18]. Imaging techniques such as positron emission tomography (PET) are
66 also limited to the measurement of one or a few compounds simultaneously [19]. Microdialysis
67 (MD) paired with mass spectrometry is the most commonly used method for measuring multiple
68 neuromodulators in awake behaving animals. MD provides a data collection method which is
69 then analyzed post hoc to identify and quantify collected analytes. It operates with a semi-
70 permeable membrane which allows for the continuous collection of the available extracellular
71 neuromodulators through passive diffusion, and can even be used to locally release

72 pharmacological agents [20–22]. However, MD does have several disadvantages including
73 disrupting the tissue during its initial placement of the probe or a guiding cannula resulting in
74 damage-induced release of neuromodulators that can last several hours before stable
75 measurements become possible. Moreover, MD has low affinity for hydrophobic compounds and
76 comparatively broad spatial and temporal resolution that is in the range of 200-400 μm in
77 diameter and 10-20 minutes, respectively. These values are dependent on the surface area of the
78 permeable membrane, the exact method of MD, flow rate, resolution of detection methods for
79 analytes of interest, tissue tortuosity and more [20–22].

80 In light of these limitations of available measurement techniques, we set out to
81 characterize a novel protocol for measuring multiple neuromodulators in vivo using probes
82 optimized for solid phase microextraction (SPME) [23]. SPME probes are thin (200 μm) wires of
83 arbitrary length coated with an inert porous polymeric matrix using biocompatible binder on one
84 end where molecules with appropriate size and affinity migrate via passive diffusion and are
85 retained by chemical interactions (*see* Methods). SPME provides an alternate method for data
86 collection which can then be analyzed by tools such as mass spectrometers. This method has
87 been shown to extract in neural tissue dynamic changes in dopamine (DA) and serotonin (5-HT)
88 levels with comparable precision to MD [24,25]. Additionally, due to the similarity of SPME
89 probes to commonly used micoelectrodes in electrophysiological recordings, relatively minor
90 adjustments will allow for the adaptation of conventional microelectrode driving systems for
91 SPME use. This, combined with post collection analysis through standard chemistry facilities
92 makes SPME an attractive and easy-to-use tool for electrophysiology labs.

93 The ability of SPME to report major neuromodulators as well as glutamate and GABA
94 were tested in two behaving rhesus macaques. Probes were repeatedly and simultaneously

95 inserted into two cortical regions and the striatum to observe inter-areal differences between
96 extracellular neuromodulator concentrations. We found that extracellular concentrations of
97 glutamate, dopamine, acetylcholine and choline could be reliably distinguished and differed
98 systematically between brain regions.
99
100 **Results**
101 During all measurements animals were engaged in a cognitively demanding task with stable
102 behavioral performance to minimize state dependent fluctuations of basal extracellular
103 concentrations of neuromodulators. Three brain regions were selected to provide a sample of
104 extracellular neuromodulatory concentrations. Two cortical regions: prefrontal cortex (PFC) area
105 8, premotor cortex (PreMC) area 6 and the head of the caudate nucleus (CD) were selected (**Fig**
106 **1F**). In 3 daily sessions, we sampled 3 times per session simultaneously from all three areas.
107 Monkey As had an additional 3 days of recording with one sample collected on each day.
108 Overall we collected and analyzed 12 probes in monkey As and 9 probes in monkey Ke. We
109 were specifically interested in major neuromodulators and neurotransmitters but successfully
110 measured other compounds such as amino acids (e.g. glutamine, taurine, phenylalanine etc) that
111 we do not discuss here.
112 To allow comparison of the SPME extraction results to those typically reported in
113 microdialysis studies, we calculated the relative change in measured concentrations across the
114 three successive sampling events per session pooled across monkeys to enhance the statistical
115 power of the analysis (**Fig 2**). Relative to the end of the first sampling event, the second and third
116 sampling events started after 40 minutes and 100 minutes respectively. We expected that the
117 variability of measurements (indexed as standard error of the median) is comparable to

118 repeatedly measured microdialysis of an identical, active brain state. We found that measured
119 concentrations did not change significantly across sampling events for any compound area
120 combination (Wilcoxon rank sum test; **Fig 2**).

121 We found that four target neurotransmitters and neuromodulators were reliably detected
122 in each animal: glutamate, dopamine, acetylcholine, and choline. Serotonin was also detected on
123 several probes but always near the limit of detection (LOD) and therefore was excluded from
124 analyses here (a report of serotonin is provided in the **Supplementary Results**) [26]. Glutamate
125 concentrations were several orders of magnitude higher than all other observed compounds of
126 interest in all areas and both animals. Relative to glutamate, choline concentrations were >15
127 times lower, DA concentrations were >700 lower and ACh concentrations were >8300 times
128 lower (**Fig 3**).

129 Glutamate concentrations (across areas) ranged from 159,147 (±19,395) to 233,659
130 ng/mL (±33,917) in monkey As, and from 135,523 (±22,945) to 184,333 ng/mL (±33,516) in
131 monkey Ke (median, SEMedian). Neither animal showed a significant difference in glutamate
132 concentrations between areas (As: kruskal-wallis test, $p = 0.063$; Ke: kruskal-wallis test, $p =$
133 0.48). However, in both monkeys, glutamate concentrations were highest in the head of the
134 caudate, which showed a trend to be higher in the caudate than in premotor cortex in monkey As
135 (Wilcoxon rank sum test, $p = 0.0226$, not significant at the Bonferroni corrected alpha level of $p=$
136 0.0167). Comparisons between monkeys showed no significant differences between the
137 glutamate concentrations in any of the measured areas (**Fig 3**).

138 In addition to glutamate, dopamine could be reliably detected in both monkeys in the
139 caudate at concentrations of 232 ng/mL (±47) in monkey As, and 226 ng/mL (±31) in monkey

140 As. These concentrations were similar between monkeys (Wilcoxon rank sum test p = 1, n.s.).
141 Dopamine was not found above detection limits in frontal cortex.

142 Acetylcholine measurements in the three brain areas ranged from (across areas) 25 (±2)
143 to 36 ng/mL (±5) in monkey As, and from 29 (±2) to 36 ng/mL (±4) in monkey Ke. Extracellular
144 ACh concentrations were significantly different between areas in monkey As (kruskal-wallis test,
145 p = 0.008). The caudate showed significantly higher concentrations than premotor cortex and a
146 trend to higher concentrations than PFC (PFC8a: Wilcoxon rank sum test, p = 0.04; PreM6:
147 Wilcoxon rank sum test, p = 0.005); only the difference between PreM6 and caudate survived
148 multiple comparisons correction (Bonferroni alpha = 0.0167). Cortical areas were not
149 significantly different from one another (Wilcoxon rank sum test, p = 0.17). In monkey Ke, only
150 one cortical region had concentrations of ACh above detection limits, which approached
151 significant difference to the concentrations measured in the caudate (Wilcoxon rank sum test, p =
152 0.08). Measurements of extracted ACh in the pre-motor cortex of monkey Ke were consistently
153 below detection limits (**Fig 3**).

154 We next measured choline which is a main product of the enzymatic breakdown of the
155 highly regulated ACh and which is a main indicator of attentional modulation of cholinergic
156 activity in frontal cortex [27]. Choline concentrations ranged across areas from 2,914 (±590) to
157 5,078 ng/mL (±675) in monkey As, and 3,408 (±3,705) to 5,533 ng/mL (±860) in monkey Ke.
158 Choline concentrations between areas were significantly different in monkey As (kruskal-wallis
159 test, p = 0.0262), but not monkey Ke (kruskal-wallis test, p = 0.25). Pairwise comparisons in
160 monkey As showed that concentrations after multiple comparison correction were significantly
161 different between PreM6 and the caudate (Wilcoxon rank sum test, p = 0.01; Bonferroni alpha =
162 0.0167), and approached significance for PFC8 *versus* caudate (Wilcoxon rank sum test, p =

163 0.06; Bonferroni alpha = 0.0167). Comparisons of choline concentrations between monkeys were
164 not significant in any of the measured areas.
165
166 **Discussion**
167 We demonstrated the reliable measurements of glutamate, dopamine, acetylcholine and choline
168 simultaneously within cortical and subcortical regions of awake and behaving macaques using
169 coated microprobes optimized for solid phase microextraction. Glutamate concentrations were
170 several orders of magnitude higher than dopamine, acetylcholine and choline across brain
171 regions. Extracellular concentrations of choline, dopamine and acetylcholine were detected at
172 >15, >700, and >8,300 times lower than glutamate respectively. Dopamine was readily detected
173 in the caudate but not observed at detectable concentrations in the cortical regions measured.
174 Acetylcholine concentrations showed a statistical trend of being different between the caudate
175 and measured cortical areas and with high consistency between monkeys. Choline
176 concentrations, a product of acetylcholine degradation as well as a precursor for its synthesis,
177 were negatively correlated with acetylcholine ($R = -0.355$; $p = 0.01$). Together, these findings
178 provide new and rare insights about the neurochemical circuit profiles during an active brain
179 state in three areas of the primate fronto-striatal network.
180 The high consistency of measured concentrations within animals, between brain areas
181 and between monkeys suggests that SPME microprobes could provide a versatile neuro-
182 technique for understanding how variations of the neurochemical milieu relate to local and long-
183 range circuit operations and ultimately cognitive functioning.
184

185 **Extracellular Concentrations of Glutamate, Dopamine, Acetylcholine and Choline.** Our
186 results revealed particularly high levels of glutamate within all measured brain regions (PFC,
187 PreMC, and CD) relative to other neuromodulators. This finding is consistent with its ubiquitous
188 role as major excitatory neurotransmitter. This holds true even in the caudate which consists
189 exclusively of GABAergic neurons, but receives glutamatergic inputs from the cortex [28].
190 Tonic concentrations of glutamate within the striatum have been previously reported to be
191 comparable to that of the hippocampus, prefrontal cortex and other cortical areas due to
192 glutamatergic inputs, extra-synaptic release and glial release [29–31]. In contrast, classical
193 neuromodulators such as DA and ACh, are released in extracellular space through volume
194 transmission where they are highly regulated and may bind to receptors on multiple neurons [32–
195 35]. This regulation may help explain the relatively low observed concentrations of DA and ACh
196 and may be a large source of extracellular choline through the enzymatic breakdown of ACh.

197 Extracellular DA was measured well above the detection threshold in the striatum. In
198 combination with glutamatergic and cholinergic concentrations, our results show promise in the
199 application of SPME to further our understanding of the relationship between glutamatergic
200 inputs to the striatum and the neuromodulatory ACh and DA signals impinging on striatal
201 circuits. Such circuits are strongly involved in hypo- and hyperkinetic diseases [3,15].
202 Dopaminergic signals did not exceed the detection threshold in either cortical regions. The
203 presence of DA in the PFC is well documented [36] and thus has failed to exceed our detection
204 limit. A possible explanation for the lack of detectable cortical DA is the susceptibility of
205 catecholamines to oxidation. This may be partially addressed by faster coupling of sample
206 collection to quantitation by MS (see **Supplementary Discussion**).

207 Few previous studies have documented ACh concentrations in vivo due to its rapid
208 breakdown by acetylcholinesterase [35,37,38]. ACh plays a major role in organizing local
209 circuits, deployment of attention, locomotion and reward through different receptors present in
210 cortical and subcortical regions [6,39,40]. It has been difficult to discern which ACh
211 concentration corresponds to efficient endogenous circuit operations. Our finding of
212 measurements in all sampling locations except for premotor cortex in monkey Ke, is therefore a
213 promising starting point for future studies comparing ACh concentrations, in conjunction with
214 other neuromodulators, during different cognitive states. The fast turn-around of ACh due to
215 AChE however, likely leads to an underestimation of ACh concentrations by SPME. Although
216 AChE cannot traverse the porous SPME coating due to its size (~7.6nm diameter), preventing
217 any enzymatic degradation of trapped ACh (**Supplementary Material**), the dynamic
218 equilibration process continuously leads to a transfer of ACh out of the SPME coating following
219 the concentration gradient of the rapidly depleted ACh into the extracellular space as discussed
220 in the case of calibration in the coating approach [41,42].

221 Amongst other sources, choline is created as a byproduct of ACh degradation by AChE.
222 Choline is also a precursor for the synthesis of ACh. Given this relationship, a negative
223 correlation between choline concentrations and ACh is expected which we indeed observed in
224 our dataset. Despite the difference in the measured concentrations of choline and acetylcholine,
225 other studies with similar differences have demonstrated the relationship of ACh and choline to
226 behavior within the cortex [27]. Future studies may focus on quantifying this relationship across
227 a wider range of brain states.

228

229 **Reliable Measurement of Individual Differences of State Specific Neuromodulatory Tone.**
230 Our results suggest that SPME probes provide reliable and sensitive measurements in
231 consecutive sampling events within an experimental session and between sessions on
232 consecutive days. These results were obtained while we controlled brain states across
233 measurement events by engaging animals in a cognitive task. This experimental control could
234 have contributed to the comparable extracellular levels of neuromodulators from sample to
235 sample within *and* between days from similar brain locations (**Fig 2**) [43–46]. The
236 reproducibility of multiple measurements at the same anatomical location within and between
237 days suggests that the SPME penetrations did not significantly disturb tissue [24]
238 (**Supplementary Information**). This conclusion contrasts with reported experience from
239 microdialysis measurements, where the initial placement of the probe or guiding cannula causes
240 transient measurement instabilities that can require several hours of settling time before reliable,
241 steady state neuromodulator concentrations are measurable [29,47–50]. These waiting periods
242 must be taken into account when designing microdialysis experiments for in vivo tracking of
243 neuromodulators during behavioral tasks in awake and restrained animals. Furthermore, the
244 reliability of observations for the reported neurochemicals with SPME is extremely high and
245 outperforms many reported microdialysis studies. We present 100% reliability in reporting
246 glutamate and choline concentrations in all brain regions and subjects. Acetylcholine
247 concentrations were reported with 100% reliability in one animal and 92% (11/12 probes) in the
248 other within the prefrontal cortex, 0% reliability (below detection threshold) in one animal and
249 83% (10/12 probes) in the other within the premotor cortex and 100% reliability in one animal
250 and 92% (11/12 probes) in the other within the caudate. Dopamine concentrations were reported

251 with 100% reliability in both animals in the caudate and were not observed above detection
252 thresholds in the cortex.
253
254 **Qualities and Advantages of SPME.** Our results illustrate several inherent advantages of using
255 SPME to measure neurochemical profiles in brain circuits [26]. As illustrated in **Table S1**,
256 SPME complements or outperforms alternative techniques in various domains. Practically, the
257 arbitrary length of the wire where the SPME coating is placed allows for robust placement within
258 the brain. The narrow diameter of the SPME probe that is within the range common to electrodes
259 for electrophysiological recordings, allows for repeated, simultaneous sampling at multiple sites
260 without observable changes to detected extracellular neuromodulator levels using 20-minute
261 sampling times.
262 *Spatial Resolution.* In principle, the spatial resolution of the SPME measurements are
263 capable of reflecting laminar concentration gradients across areas as small as several tens of
264 micrometers. In our protocol we coated 3mm in length with 50 μm of thickness and desorbed the
265 entire area into an organic solvent mixture for subsequent LC-MS/MS analysis. However, with
266 the use of other techniques, such as desorption electrospray ionization (DESI), which represents
267 a direct-to-MS approach [51], much smaller areas of the SPME matrix may be analyzed at a time
268 allowing for laminar or near-laminar resolution. Direct coupling of SPME fibres to MS is the
269 preferred mode, as it provides the most rapid analysis thus preventing diffusion of compounds
270 within the coating and smearing the imprinted layer information. If diffusion of molecules within
271 the fibre is high, it can be prevented by, for example, the inclusion of a divider between two
272 halves of the coating. This would allow the simultaneous measurement of separated
273 compartments of a cortical column. The absolute spatial resolution of SPME is difficult to

274 estimate as SPME operates through diffusion and dynamic equilibration similar to MD. As a
275 consequence, the sampled volume will depend on sampling time, the compound's diffusion
276 coefficient, as well as the target tissue and its properties affecting the rate of diffusion such as
277 tortuosity [32].

278 *Temporal Resolution.* Several factors determine the appropriate extraction time using
279 SPME. Depending on the goals of an experimenter, resolutions below 5 minutes may be
280 achieved as the detection limit is reached within the first few minutes for most compounds tested
281 (**Fig 1D-E**). As sampling continues, the SPME coating will eventually reach an equilibrium point
282 with the external environment (**Fig 1D-E**). In principle, sampling times beyond a stable
283 equilibrium point will result in the same extracted values of compounds. However, in the brain
284 there is no single stable equilibrium point and thus, even with long sampling times, there will be
285 some variation in extracted concentrations. Within the dynamic regime, we can still calculate
286 environmental concentrations from which sampling occurred given knowledge of the extraction
287 time and the dynamic range. The lower limit of this dynamic range that can be informative is
288 determined by the coating's physicochemical characteristics and sample's properties and in
289 practice also volume of desorption and sensitivity of the MS. The analytical technique's
290 sensitivity also practically determines the thickness of the SPME coating as thinner coatings
291 could in principle increase temporal resolution but would extract less compounds overall
292 requiring higher sensitivity to detect. With higher sensitivity, less time is required for the thin
293 coating to extract sufficient amounts to exceed limits of detection and quantitation. This then
294 means that the compound with regards to which the sensitivity is the lowest, limits the temporal
295 resolution because it will have the slowest-to-reach detectable concentration. However, making
296 measurements in the dynamic range requires consistency of extraction times as differences in

297 time will lead to variations of extraction yields in a range that can be estimated from the SPME
298 extraction time profiles (**Fig 1D-E**). Given the dynamic nature of brain networks and the lack of
299 a stable equilibrium point, we expect consistency in brain states to be one of the biggest factors
300 in reducing replicated variability. Moreover, SPME measurements are inherently an average of
301 the temporal dynamics of the target tissue milieu. This means that due to the bi-directional
302 exchange of neuromodulators from the extracellular space and the SPME coating, longer periods
303 of stable concentration gradients will be more strongly reflected in the extracted measurements.

304 *Utility and Ease of Use.* SPME based microprobe extraction allows for multiple
305 simultaneous measurements that can be reliably repeated within the same measurement sessions
306 at the same locations with no evidence of damage induced disruption of the neurochemical
307 environment. Another critical advantage of SPME over comparable MS-analysis based methods
308 such as MD is its ease of use and accessibility. Due to their similar size to recording
309 microelectrodes used for electrophysiology, little adjustment is required for conducting SPME
310 measurements using existing acute microelectrode positioning systems. Measurements in deeper
311 structures should use an accompanying guide tube (**Fig 1C**) as travelling through non-target
312 tissue will result in unwanted chemical collection. Beyond the collection, a chemistry core could
313 apply LC-MS/MS to the probes allowing for relatively easy quantitation of extracellular
314 compounds of interest.

315 *Detection Methods.* SPME is ultimately a sampling method, much like MD, that provides
316 data for analytical tools such as chromatography and mass spectrometry. In fact, once SPME
317 analytes have been desorbed from the probe into a solvent, data provided by SPME and MD are
318 treated very much the same. Thus, the advancement in detection limits and reliability of post-hoc
319 analytical methods utilized by MD also benefit SPME, and vice versa. However, SPME sample

320 analysis is more reliably and conveniently coupled to LC-MS/MS as it lacks issues such as high
321 salt content of collected dialysate that MD suffers from [52].

322 *Extension of SPME measurements beyond classical neuromodulators*. A unique
323 advantage of SPME over alternative methods of in vivo detection of compounds within the brain
324 is its potential affinity for hydrophobic compounds. Although MD is capable of collecting
325 metabolomics data similarly to SPME [20,53,54], the artificial cerebra-spinal fluid that is
326 commonly traversing the semi-permeable membrane better facilitates the collection of
327 hydrophilic molecules. This means that molecules that cross the semi-permeable membrane and
328 are therefore collected and quantified through LC-MS are much more likely to be hydrophilic.
329 SPME, in contrast, provides balanced analyte coverage, which means that in principle certain
330 SPME matrix coatings have similar affinity for both hydrophilic or hydrophobic compounds
331 [55]. Data collected here includes other neurochemicals of interest such as amino acids (e.g.
332 glutamine, taurine, phenylalanine, etc) that we reliably detected but do not discuss here. In
333 practice, the detection of very polar molecules such as monoamines and catecholamines requires
334 coating chemistry that facilitates hydrophilic compound extraction. Comparatively many lipids
335 play important roles in intracellular signaling and have been suggested to provide biomarkers for
336 psychiatric disorders [56,57], therefore making SPME a potentially versatile and comprehensive
337 tool for brain neurochemistry studies.

338

339 **Implications for Understanding and Treating Psychiatric Disease States.** Most psychiatric
340 disorders are accompanied by neuromodulatory dysregulation [3]. However, this fact is seldom
341 studied in a multi-modulatory manner with a single or few nuclei or neurochemicals being
342 observed at a time. This is an increasingly evident problem because models attributing symptoms

343 of a disorder to a single neuromodulator often fall short in explaining many symptoms [13,14].
344 For example, in Parkinson's disease, outside of the well characterized dopaminergic deficits,
345 there is evidence for deficits in noradrenergic, cholinergic and serotonergic systems as well
346 [6,15,58]. Many cognitive deficits observed within Parkinson's disease are linked to such non-
347 dopaminergic deficits. Such findings emphasize the need to simultaneously observe multiple
348 neuromodulatory systems. Thus the simultaneous measurement of multiple neuromodulators, in
349 multiple brain regions within healthy and clinical populations will allow for a better
350 understanding of the underlying causes of symptoms and progression of psychiatric disorders
351 [3,4,59].

352 A better understanding of psychiatric disorders through multi-modulator methods may
353 also lead to more accurate understanding of the action of pharmacological agents. Previously,
354 many studies aimed at identifying the locus of action of a pharmacological agent have used local
355 injection methods such as iontophoresis or microinjections [60,61]. Although highly informative
356 about the role of neuromodulators in modulating the activity of individual cells and circuits, this
357 approach does not allow physiologically realistic exploration of a systemically administered
358 pharmacological agent. Pharmacological agents are often administered in some systemic fashion
359 and even with highly specific receptor affinities, may interact with multiple neuromodulatory
360 systems through the actions of heteroreceptors [4,5,62]. Multi-modulator measurements, as
361 described here, will allow for a better understanding of pharmacological agents, as well as
362 provide novel insights into the development of more effective drugs or combinations of drugs to
363 better treat the clinical population.
364

365 **Conclusion**. We described a novel SPME protocol capable of simultaneous, multi-modulator
366 measurements of multiple brain regions. Our results suggest that SPME both supplements
367 current methods of neuromodulator detection and allows for novel measurements previously not
368 possible for the investigation and dissection of neuromodulatory systems, their role in
369 physiological brain processes and their modulation by pharmacological agents.
370

371 **Methods**

372 **Animals**

373 Data was collected from two 8 year-old male rhesus macaques (*Macaca mulatta*) weighing 8-12
374 kg. All animal care and experimental protocols were approved by the York University Animal
375 Care Committee and were in accordance with the Canadian Council on Animal Care guidelines.
376 Details regarding the experimental setup, recording procedures, and reconstruction of recording
377 sites have been described previously [63]. Briefly, animals were implanted with a 20 mm by 28
378 mm recording chamber over the frontal region of the right hemisphere guided by stereotaxic
379 coordinates [64] and MR images. The animals were seated in a custom made primate chair and
380 head stabilized with their eyes 65cm away from a 21' LCD monitor refreshed at 85 Hz. Eye
381 traces were collected by a video-based eye-tracking system (Eyelink 1000 Osgoode, Ontario,
382 Canada, 500 Hz sampling rate). The animals were engaged in an over-trained attention tasks in
383 which they would use saccadic eye movements to acquire juice reward. The specifics of the task
384 are described elsewhere [65]. Both animals showed stable performance and acquired similar
385 reward volumes on all recording days. In both tasks, stimulus presentation and reward delivery
386 was controlled through MonkeyLogic (http://www.brown.edu/Research/monkeylogic/).
387

388 **SPME protocol and Fabrication of SPME Probes**

389 We provide a visual overview of the complete SPME protocol used here in **Fig S1** and delineate
390 the chemical materials, LC-MS/MS analysis, and detailed quantitation of neuromodulators in the
391 ***Supplementary Methods*** and in a companion paper [26]. All measurements used miniaturized
392 SPME probes that were manufactured by repeated dip-coating of stainless steel wires in a
393 suspension of extracting phase in a binder. This general procedure reported previously [66], has
394 been modified to fit the purpose of *in vivo* brain sampling [26]. The 3 mm long tip of the wire
395 was acid-etched down to approx. 100 μm to create a recession capable of accommodating thicker
396 layer of coating without significantly increasing the total probe diameter. The extracting phase
397 was an in-house synthesized hydrophilic-lipophilic balance polymer functionalized with
398 benzenesulfonic acid to introduce strong cation exchange properties (HLB-SCX). The
399 monodispersed polymeric particles with diameter of approx. 1 μm were suspended in the binder
400 consisting of 7% polyacrylonitrile dissolved in N,N-dimethylformide (w/v), ensuring the
401 particles-to-binder ratio at 15% (w/v). The extracting phase suspension was prepared one day
402 before the probe coating, homogenized by sonication and stirred at 800 rpm overnight. Several
403 layers of coating were deposited on the modified wires, resulting in total coating thickness of
404 ≈50 μm and total probe diameter of 195 μm. The average pore size of the extracting phase was
405 measured at 1.2nm. Before the use, the probes were cleaned with the mixture of methanol,
406 acetonitrile and 2-propanol (50:25:25, v/v/v), activated in the mixture of methanol and water
407 (50:50. v/v) and sterilized in steam for 15 min at 121°C. During the sampling, SPME probes
408 were inserted into sheathing cannulas to protect the coating and prevent it from extracting
409 compounds on the way to the target brain area. The cannulas underwent the same cleaning and

410 sterilization procedure as the probes and then the lengths of both components of the SPME
411 assembly were adjusted to 60-70 and 70-80 mm for the probes and cannulas, respectively.
412

413 **MRI Guided Electrophysiological Mapping of Target Tissue**

414 The anatomical coordinates of the brain regions of interest were first identified through 3 T MR
415 images. The MR images were then verified with extracellular electrophysiological recordings of
416 the target areas, which provided the gray and white matter boundaries for the cortical sites and
417 the dorsal most aspect of the head of the caudate nucleus. Tungsten microelectrodes were 200
418 μm thick with an impedance of 1-2 MΩ. All electrodes, SPME probes and their accompanying
419 guiding cannulas were driven down into the brain and later out using software-controlled
420 precision microdrives (Neuronitek, ON, Canada). Electrodes were connected to a multichannel
421 acquisition processor (Neuralynx Digital Lynx system, Inc., Bozeman, Montana, USA) which
422 was used for data amplification, filtering and acquisition of spiking activity. Spiking activity was
423 obtained by applying a 600-8000 Hz bandpass filter, with further amplification and digitization
424 at a 32 KHz sampling rate. For every recording day, electrodes were lowered until the first
425 detection of spiking activity (indicative of gray matter) at the depth suggested by the MR images.
426

427 **SPME Sampling and Post-Processing Procedures**

428 All three SPME assemblies (example of sampling using one assembly in **Fig 1A-C**) were
429 simultaneously driven to 200 μm above the point of first spiking detection. SPME assemblies
430 were located ~1 mm away from the electrode penetration location. Then, only the SPME probes
431 were inserted 3 mm into the areas of interest. On average macaque cortical thickness is only 2
432 mm while the head of the caudate at the point of sampling was well over 3 mm. An extraction

433 duration of 20 min was selected to reflect stable extraction time profiles for all compounds of
434 interest. Extraction time profiles reflect the detectable concentration of collected analyte over
435 time, which is captured in sequence by a linear "kinetic" regime, a "dynamic" regime and an
436 "equilibrium" regime over extraction time. We illustrate in **Fig 1D-E** these regimes for two main
437 compounds measured with the SPME probe we used in vivo. After the 20 min extraction event,
438 all SPME probes were driven back 3 mm into the guiding cannulas and all SPME assemblies
439 were withdrawn from the brain (**Fig 1A-C**).

440 The microdrives were removed from the chamber to enable unclamping of the SPME
441 probes, a brief wash and then storage in glass vials surrounded by dry ice until placing them into
442 a -80°C freezer. One entire sampling event (one extraction in 3 different brain areas together
443 with assembling the SPME probes and cannulas, driving into and out of brain, washing and
444 preparing for storage) was performed within 50 min, except for the first sampling event in each
445 sampling day. The first sampling event, with the area identification using electrophysiology
446 recording, was performed within 75 min.

447 **Neuromodulators detection and quantitation**

448 Detection and quantitiation of neuromodulators followed previously established procedures
449 described in the **Supplementary Material**. In brief, SPME probes were defrosted and desorbed
450 in an aqueous solution containing water, acetonitrile, methanol, formic acid and deuterated
451 isotopologues of target neuromodulators as internal standards (IS). Chromatographic separation
452 of target compounds was conducted as previously reported [25]. Tandem mass spectrometry
453 (MS/MS) was performed with electrospray ionization with two MS/MS transitions for each
454 neuromodulator and one for each IS [26].

455 Stock solutions of all target neuromodulators were prepared and used to generate
456 standard calibration curves and to calculate the amounts of neuromodulator extracted by each
457 experimental SPME probe. Conversion of the amount of neuromodulator extracted to in-brain
458 concentrations was done using matrix-matched external calibrations. LOD is defined as 3 times
459 the signal obtained from blank samples.

460
461

462 **Acknowledgments**

463 This research was supported by grants from the Canadian Institutes of Health Research (CIHR),
464 the Natural Sciences and Engineering Research Council of Canada (NSERC) and the Ontario
465 Ministry of Economic Development and Innovation (MEDI). We thank Dr. Hongying Wang for
466 invaluable help with animal care. We thank Thermo Scientifc for providing the triple quadrupole
467 mass spectrometer TSQ Quantiva used in this work as a loan to our laboratory. The authors
468 thankfully acknowledge Pfizer Canada Inc., Merck Canada Inc., Quebec Consortium for Drug
469 Discovery (CQDM), Brain Canada, and Ontario Brain Institute for the grant "Solid phase
470 microextraction-based integrated platform for untargeted and targeted in vivo brain studies".

471 **Conflicts of interest**

472 None of the authors have any conflict to disclose.

473 **References**
474

475 1. Thiele A, Bellgrove MA. Neuromodulation of Attention. Neuron. Elsevier Inc.; 2018;97:
476 769–785. doi:10.1016/j.neuron.2018.01.008
477 2. Marder E. Overview Neuromodulation of Neuronal Circuits: Back to the Future. Neuron.
478 Elsevier Inc.; 2012;76: 1–11. doi:10.1016/j.neuron.2012.09.010
479 3. Millan MJ, Agid Y, Brüne M, Bullmore ET, Carter CS, Clayton NS, et al. Cognitive
480 dysfunction in psychiatric disorders: characteristics, causes and the quest for improved
481 therapy. Nat Rev Drug Discov. Nature Publishing Group; 2012;11: 141–168.
482 doi:10.1038/nrd3628
483 4. Avery MC, Krichmar JL. Neuromodulatory Systems and Their Interactions : A Review of
484 Models , Theories , and Experiments. Front Neural Circuits. 2017;11: 1–18.
485 doi:10.3389/fncir.2017.00108
486 5. Gobert A, Audinot V, Cistarelli L, Millan MJ. Simultaneous quantification of serotonin,
487 dopamine and noradrenaline levels in single frontal cortex dialysates of freely-moving rats
488 reaveals a complex pattern of reciprocal auto- and heteroreceptor-mediated control of
489 release. Neuroscience. 1998;84: 413–429.
490 6. Moehle MS, Pancani T, Byun N, Yohn SE, Wilson GH, Dickerson JW, et al. Cholinergic
491 Projections to the Substantia Nigra Pars Reticulata Inhibit Dopamine Modulation of Basal
492 Ganglia through the M4Muscarinic Receptor. Neuron. 2017;96: 1358–1372.
493 doi:10.1016/j.neuron.2017.12.008
494 7. Santana N, Mengod G, Artigas F. Expression of a1-adrenergic receptors in rat prefrontal
495 cortex: cellular co-localization with 5-HT2A receptors. Int J Neuropsychopharmacol.
496 2018;16: 1139–1151. doi:10.1017/S1461145712001083
497 8. Arnsten AFT, Paspalas CD, Gamo NJ, Yang Y, Wang M. Dynamic network connectivity:
498 A new form of neuroplasticity. Trends Cogn Sci. Elsevier Ltd; 2010;14: 365–375.
499 doi:10.1016/j.tics.2010.05.003
500 9. Hassan SF, Zumut S, Burke PG, Mcmullan S, Cornish JL, Goodchild AK. Comparison of
501 noradrenlaine, dopamine and serotonin in mediating the tachycardic and thermogenic
502 effects of methamphetamine in the ventral medial prefrontal cortex. Neuroscience. IBRO;
503 2015;295: 209–220. doi:10.1016/j.neuroscience.2015.03.028
504 10. Wang JKT, Andrews H, Thukral V. Presynaptic Glutamate Receptors Regulate
505 Noradrenaline Release from Isolated Nerve Terminals. J Neurochem. 1992;58: 204–211.
506 11. Ghersi C, Bonfanti A, Manzari B, Feligioni M, Raiteri M, Pittaluga A. Pharmacological
507 heterogeneity of release-regulating presynaptic AMPA / kainate receptors in the rat brain :
508 study with receptor antagonists. Neurochem Int. 2003;42: 283–292.
509 12. Pittaluga A, Feligioni M, Longordo F, Luccini E, Raiteri M. Trafficking of presynaptic
510 AMPA receptors mediating neurotransmitter release : Neuronal selectivity and
511 relationships with sensitivity to cyclothiazide. Neuropharmacology. 2006;50: 286–296.
512 doi:10.1016/j.neuropharm.2005.09.004
513 13. Bohnen NB, Albin R, Muller MLTM, Petrou M, Kotagal V, Koeppe RA, et al. Frequency
514 of Cholinergic and Caudate Nucleus Dopaminergic Deficits Across the Predemented
515 Cognitive Spectrum of Parkinson Disease and Evidence of Interaction Effects. JAMA
516 Neurol. 2015;72: 194–200. doi:10.1001/jamaneurol.2014.2757
517 14. Remy P, Doder M, Lees A, Turjanski N, Brooks D. Depression in Parkinson ' s disease:
518 loss of dopamine and noradrenaline innervation in the limbic system. Brain. 2005;128:

519 1314–1322. doi:10.1093/brain/awh445
520 15. Halliday GM, Leverenz JB, Schneider JS, Adler CH. The Neurobiological Basis of
521 Cognitive Impairment in Parkinson's Disease. Mov Disord. 2014;29: 634–650.
522 doi:10.1002/mds.25857
523 16. Jacobs CB, Peairs MJ, Venton BJ. Review: Carbon nanotube based electrochemical
524 sensors for biomolecules. Anal Chim Acta. 2010;662: 105–127.
525 doi:10.1016/j.aca.2010.01.009
526 17. Dale N, Hatz S, Tian F, Llaudet E. Listening to the brain: Microelectrode biosensors for
527 neurochemicals. Trends Biotechnol. 2005;23: 420–428. doi:10.1016/j.tibtech.2005.05.010
528 18. Vartak D, Togt C Van Der, Vugt B Van, Roelfsema PR. Electrochemical measurement of
529 acetylcholine in the dorsolateral prefrontal cortex : A technical report. BioRXiv. 2017; 1–
530 25.
531 19. Fisher RE, Morris ED, Alpert NM, Fischman AJ. In Vivo Imaging of Neuromodulatory
532 Synaptic Transmission Using PET : A Review of Relevant Neurophysiology. Hum Brain
533 Mapp. 1995;3: 24–34. doi:https://doi.org/10.1002/hbm.460030104
534 20. Anderzhanova E, Wotjak CT. Brain microdialysis and its applications in experimental
535 neurochemistry. Cell Tissue Res. 2013;354: 27–39. doi:10.1007/s00441-013-1709-4
536 21. Watson CJ, Venton BJ, Kennedy RT. In Vivo Measurements of Neurotransmitters by
537 Microdialysis Sampling. Anal Chem. 2006;78: 1391–1399. doi:10.1021/ac0693722
538 22. Kennedy RT. Emerging trends in in vivo neurochemical monitoring by microdialysis.
539 Curr Opin Chem Biol. Elsevier Ltd; 2013;17: 860–867. doi:10.1016/j.cbpa.2013.06.012
540 23. Pawliszyn J. Theory of Solid-Phase Microextraction. In: Pawliszyn J, editor. Handbook of
541 Solid Phase Microextraction. Elsevier; 2012. pp. 13–59.
542 24. Cudjoe E, Bojko B, de Lannoy I, Saldivia V, Pawliszyn J. Solid-Phase Microextraction: A
543 Complementary In Vivo Sampling Method to Microdialysis. Angew Chemie Int Ed.
544 2013;52: 12124–12126. doi:10.1002/anie.201304538
545 25. Cudjoe E, Pawliszyn J. Optimization of solid phase microextraction coatings for liquid
546 chromatography mass spectrometry determination of neurotransmitters. J Chromatogr A.
547 Elsevier B.V.; 2014;1341: 1–7. doi:10.1016/j.chroma.2014.03.035
548 26. Lendor S, Hassani S-A, Boyaci E, Singh V, Womelsdorf T, Pawliszyn J. Development of
549 solid phase microextraction-based miniaturized probe and protocol for extraction of
550 neurotransmitters from brain in vivo.
551 27. Parikh V, Kozak R, Martinez V, Sarter M. Prefrontal Acetylcholine Release Controls Cue
552 Detection on Multiple Timescales. Neuron. 2007;56: 141–154.
553 doi:10.1016/j.neuron.2007.08.025
554 28. Haber SN, Knutson B. The reward circuit: Linking primate anatomy and human imaging.
555 Neuropsychopharmacology. Nature Publishing Group; 2010;35: 4–26.
556 doi:10.1038/npp.2009.129
557 29. Moussawi K, Riegel A, Nair S, Kalivas PW, Bargas J, Nacional U. Extracellular
558 glutamate : functional compartments operate in different concentration ranges. Front Syst
559 Neurosci. 2011;5: 1–9. doi:10.3389/fnsys.2011.00094
560 30. Moghaddam B. Stress Preferentially Increases Extraneurona Levels of Excitatory Amino
561 Acids in the Prefrontal Cortex : Comparison to Hippocampus and Basal Ganglia. J
562 Neurochem. 1993;60: 1650–1657.
563 31. Ascenzo MD, Fellin T, Terunuma M, Revilla-sanchez R, Meaney DF, Auberson YP, et al.
564 mGluR5 stimulates gliotransmission in the nucleus accumbens. Proc Natl Acad Sci.

565 2006;104: 1995–2000.
566 32. Syková E. Extrasynaptic volume transmission and diffusion parameters of the
567 extracellular space. Neuroscience. 2004;129: 861–876.
568 doi:10.1016/j.neuroscience.2004.06.077
569 33. Vizi ES. Role of high-affinity receptors and membrane transporters in nonsynaptic
570 communication and drug action in the central nervous system. Pharmacol Rev. 2000;52:
571 63–89.
572 34. Santello M, Calì C, Bezzi P. Gliotransmission and the Tripartite Synapse. In: Kreutz M,
573 Sala C, editors. Synaptic Plasticity Advances in Experimental Medicine and Biology.
574 2012. pp. 307–331.
575 35. Schwartz J, Javitch J. Neurotransmitters. In: Kandel E, Schwartz J, Jessell T, Siegelbaum
576 S, Hudspeth A, editors. Principles of Neural Science. 2013. pp. 289–306.
577 36. Goldman-Rakic PS, Lidow MS, Gallager DW. Overlap of dopaminergic, adrenergic, and
578 serotoninergic receptors and complementarity of their subtypes in primate prefrontal
579 cortex. J Neurosci. 1990;10: 2125–2138.
580 37. Kreitzer AC. Physiology and pharmacology of striatal neurons. Annu Rev Neurosci.
581 2009;32: 127–47. doi:10.1146/annurev.neuro.051508.135422
582 38. Zapata A, Chefer VI, Parrot S, Denoroy L. Detection and Quantification of
583 Neurotransmitters in Dialysates. Curr Protoc Neurosci. 2013;63: 1–35.
584 doi:10.1002/0471142301.ns0704s63
585 39. Granger AJ, Mulder N, Saunders A, Sabatini BL. Cotransmission of acetylcholine and
586 GABA. Neuropharmacology. Elsevier Ltd; 2016;100: 40–46.
587 doi:10.1016/j.neuropharm.2015.07.031
588 40. Howe WM, Gritton HJ, Lusk NA, Roberts EA, Hetrick VL, Berke JD, et al. Acetylcholine
589 Release in Prefrontal Cortex Promotes Gamma Oscillations and Theta–Gamma Coupling
590 during Cue Detection. J Neurosci. 2017;37: 3215–3230. doi:10.1523/JNEUROSCI.2737-
591 16.2017
592 41. Zhang X, Es-haghi A, Musteata FM, Ouyang G, Pawliszyn J. Quantitative in Vivo
593 Microsampling for Pharmacokinetic Studies Based on an Integrated Solid-Phase
594 Microextraction System. Anal Chem. 2007;79: 4507–4513. doi:10.1021/ac070177c
595 42. Alam N, Pawliszyn J. Numerical Simulation and Experimental Validation of Calibrant-
596 Loaded Extraction Phase Standardization Approach. Anal Chem. 2016;88: 8632–8639.
597 doi:10.1021/acs.analchem.6b01802
598 43. Marder E, O'Leary T, Shruti S. Neuromodulation of Circuits with Variable Parameters:
599 Single Neurons and Small Circuits Reveal Principles of State-Dependent and Robust
600 Neuromodulation. Annu Rev Neurosci. 2014;37: 329–346. doi:10.1146/annurev-neuro-
601 071013-013958
602 44. McGinley MJ, Vinck M, Reimer J, Batista-Brito R, Zagha E, Cadwell CR, et al. Waking
603 State: Rapid Variations Modulate Neural and Behavioral Responses. Neuron. Elsevier
604 Inc.; 2015;87: 1143–1161. doi:10.1016/j.neuron.2015.09.012
605 45. Reimer J, Froudarakis E, Cadwell CR, Yatsenko D, Denfield GH, Tolias AS. Pupil
606 Fluctuations Track Fast Switching of Cortical States during Quiet Wakefulness. Neuron.
607 Elsevier Inc.; 2014;84: 355–362. doi:10.1016/j.neuron.2014.09.033
608 46. Reimer J, McGinley MJ, Liu Y, Rodenkirch C, Wang Q, McCormick DA, et al. Pupil
609 fluctuations track rapid changes in adrenergic and cholinergic activity in cortex. Nat
610 Commun. Nature Publishing Group; 2016;7: 1–7. doi:10.1038/ncomms13289

611 47. Watanabe M, Kodama T, Hikosaka K. Increase of Extracellular Dopamine in Primate
612 Prefrontal Cortex During a Working Memory Task. J Neurophysiol. 1997;78: 2795–2798.
613 doi:https://doi.org/10.1152/jn.1997.78.5.2795
614 48. Kodama T, Hikosaka K, Honda Y, Kojima T, Tsutsui K, Watanabe M. Dopamine and
615 glutamate release in the anterior default system during rest : A monkey microdialysis
616 study. Behav Brain Res. Elsevier B.V.; 2015;294: 194–197.
617 doi:10.1016/j.bbr.2015.08.013
618 49. Kodama T, Kojima T, Honda Y, Hosokawa T, Tsutsui K, Watanabe M. Oral
619 Administration of Methylphenidate (Ritalin) Affects Dopamine Release Differentially
620 Between the Prefrontal Cortex and Striatum: A Microdialysis Study in the Monkey. J
621 Neurosci. 2017;37: 2387–2394. doi:10.1523/JNEUROSCI.2155-16.2017
622 50. Kodama T, Hikosaka K, Watanabe M. Differential changes in glutamate concentration in
623 the primate prefrontal cortex during spatial delayed alternation and sensory-guided tasks.
624 Exp Brain Res. 2002;145: 133–141. doi:10.1007/s00221-002-1084-y
625 51. Deng J, Yang Y, Wang X, Luan T. Strategies for coupling solid-phase microextraction
626 with mass spectrometry. TrAC - Trends Anal Chem. Elsevier Ltd; 2014;55: 55–67.
627 doi:10.1016/j.trac.2013.12.004
628 52. Guihen E, Connor WTO. Current separation and detection methods in microdialysis the
629 drive towards sensitivity and speed. Electrophoresis. 2009;30: 2062–2075.
630 doi:10.1002/elps.200900039
631 53. Li J, von Pföstl V, Zaldivar D, Zhang X, Logothetis NK, Rauch A. Measuring multiple
632 neurochemicals and related metabolites in blood and brain of the rhesus monkey by using
633 dual microdialysis sampling and capillary hydrophilic interaction chromatography-mass
634 spectrometry. Anal Bioanal Chem. 2012;402: 2545–2554. doi:10.1007/s00216-011-5427-
635 z
636 54. Zhang X, Rauch A, Lee H, Xiao H, Rainer G, Logothetis N. Capillary hydrophilic
637 interaction chromatography/mass spectrometry for simultaneous determination of multiple
638 neurotransmitters in primate cerebral cortex. Rapid Commun Mass Spectrom. 2007;21:
639 3621–3628.
640 55. Reyes-garcés N, Gionfriddo E, Gómez-Ríos GA, Alam MN, Boyaci E, Bojko B, et al.
641 Advances in Solid Phase Microextraction and Perspective on Future Directions. Anal
642 Chem. 2018;90: 302–360. doi:10.1021/acs.analchem.7b04502
643 56. Tamiji J, Crawford A. The Neurobiology of Lipid Metabolism in. Eur PMC. 2011;18: 98–
644 112. doi:10.1159/000323189
645 57. Yehuda S, Rabinovitz S, Mostofsky DI. Mini-Review Essential Fatty Acids Are Mediators
646 of Brain Biochemistry and Cognitive Functions. J Neurosci Res. 1999;56: 565–570.
647 58. Halliday GM, Li YW, Blumbergs PC, Joh TH, Cotton PRGH, Howe PRC, et al.
648 Neuropathology of Immunohstochemically Idendied Brainstem Neurons in Parkinson's
649 Disease. Am Neurol Assoc. 1990;27: 373–385.
650 59. Anderzhanova E, Wotjak CT. NextGen Brain Microdialysis : Applying Modern
651 Metabolomics Technology to the Analysis of Extracellular Fluid in the Central Nervous
652 System. Mol Neuropsychiatry. 2015;1: 60–67. doi:10.1159/000381855
653 60. Wang M, Ramos BP, Paspalas CD, Shu Y, Simen A, Duque A, et al. alpha2A-
654 Adrenoceptors Strengthen Working Memory Networks by Inhibiting cAMP-HCN
655 Channel Signaling in Prefrontal Cortex. Cell. 2007;129: 397–410.
656 doi:10.1016/j.cell.2007.03.015

61. Lapiz MDS, Morilak DA. Noradrenergic modulation of cognitive function in rat medial prefrontal cortex as measured by attentional set shifting capability. Neuroscience. 2006;137: 1039–1049. doi:10.1016/j.neuroscience.2005.09.031
62. Millan MJ, Goodwin GM, Meyer-lindenberg A, Ove S. Learning from the past and looking to the future : Emerging perspectives for improving the treatment of psychiatric disorders. Eur Neuropsychopharmacol. 2015;25: 599–656. doi:10.1016/j.euroneuro.2015.01.016
63. Oemisch M, Westendorff S, Oemisch M, Westendorff S, Everling S, Womelsdorf XT. Interareal Spike-Train Correlations of Anterior Cingulate and Dorsal Prefrontal Cortex during Attention Shifts Interareal Spike-Train Correlations of Anterior Cingulate and Dorsal Prefrontal Cortex during Attention Shifts. J Neurosci. 2015;35: 13076–13089. doi:10.1523/JNEUROSCI.1262-15.2015
64. Paxinos G, Huang X, Toga A. The Rhesus Monkey Brain in Stereotaxic Coordinates. 2000.
65. Hassani SA, Oemisch M, Balcarras M, Westendorff S, Ardid S, van der Meer MA, et al. A computational psychiatry approach identifies how alpha-2A noradrenergic agonist Guanfacine affects feature-based reinforcement learning in the macaque. Sci Rep. Nature Publishing Group; 2017;7: 40606. doi:10.1038/srep40606
66. Gómez-Ríos GA, Tascon M, Reyes-garcés N, Boyacı E. Quantitative analysis of biofluid spots by coated blade spray mass spectrometry , a new approach to rapid screening. Sci Rep. 2017;7: 1–7. doi:10.1038/s41598-017-16494-z

680 **Fig 1. SPME sampling procedure, extraction time profiles and measurement locations**.
681 (A) Dimensions of the SPME probe and the accompanying cannula. There was a 3000 µm buffer
682 from the opening of the cannula and the start of the SPME coating. The SPME coating was 195
683 µm at the tip. The SPME coating made up the terminal 3000 µm of the entire probe and was
684 placed in a cannula with an internal diameter of 200 µm and an external diameter of 270 µm. **(**B)
685 Tungsten microelectrodes were lowered into the brain guided by 3 T magnetic resonance (MR)
686 images in order to map the depth at which detectable spiking was observed matching
687 expectations from the MR images. (C) SPME probes and their accompanying cannulas in all
688 brain areas were then simultaneously lowered to 200 µm above the point of first observable
689 firing in the target brain region and the SPME probes were lowered to expose only the 3000 µm
690 SPME coating. After 20 minutes of extraction, the SPME probes were then retracted 3000 µm
691 back into the cannula and the probes plus their accompanying cannulas were removed from the
692 brain. The table inset into the figure provides the velocities and times of each probe and cannula
693 as they transitioned between the extraction steps. (D) Extraction quantities of Glutamate in ng
694 and (E) Dopamine in ng over time. The linear "kinetic" regime and "equilibrium" regime are
695 labelled with the dynamic range being in between. (F**)** Anatomical locations of SPME sampling
696 events in the right hemisphere of two Rhesus Macaques. Target brain regions are highlighted in
697 red and include two cortical regions, prefrontal cortex (PFC) area 8 and premotor cortex (PreM)
698 area 6 as well as a subcortical region: the head of the caudate.
699
700 **Fig 2.** Changes in the normalized concentrations of the observed neuromodulators across daily
701 sampling sessions in each sampled brain region. The median concentration of (A) Glutamate (B)
702 acetylcholine (C) choline and dopamine (D) with standard error of the median plotted for each
703 sampling time and location. Data was normalization for each subject separately and for the
704 respective neurochemical and area combinations. Sampling locations are represented by different
705 lines: solid line for the prefrontal cortex, dashed line for the premotor cortex and dotted line for
706 the caudate nucleus. Sampling events were 20 minutes in length and the time between the end of
707 one sampling event to the start of the next sampling event was 40 minutes (STD 2 minutes)
708 making the second sampling event 40 minutes and the third 100 minutes from the initial
709 measurement. No significant change was observed for any neuromodulator in any brain region
710 (Wisconsin rank sum test). Note that a single prefrontal choline data point was excluded in this
711 analysis for being >4 standard deviations from the median (data point is present in **Fig 3a**).
712
713 **Fig 3. SPME sampling of the macaque brain.**
714 SPME probes extract from the cortex (PFC and PreM6) as well as the caudate of two adult
715 macaques after 20 minutes of extraction within the respective brain region. Average of n= 12
716 probes for animal As and n= 9 probes for animal Ke. Four neuromodulators were reliably
717 measured: glutamate, dopamine, acetylcholine, and choline (orange, green, purple, red
718 respectively). All brain regions had high concentrations of glutamate and relatively much lower
719 concentrations of acetylcholine and choline extracted (with the exception of animal Ke PreM6
720 lacking detectable acetylcholine). The only tested region to yield measurable dopamine was the
721 caudate. The dashed blue line depicts the limit of detection (LOD).
722
723

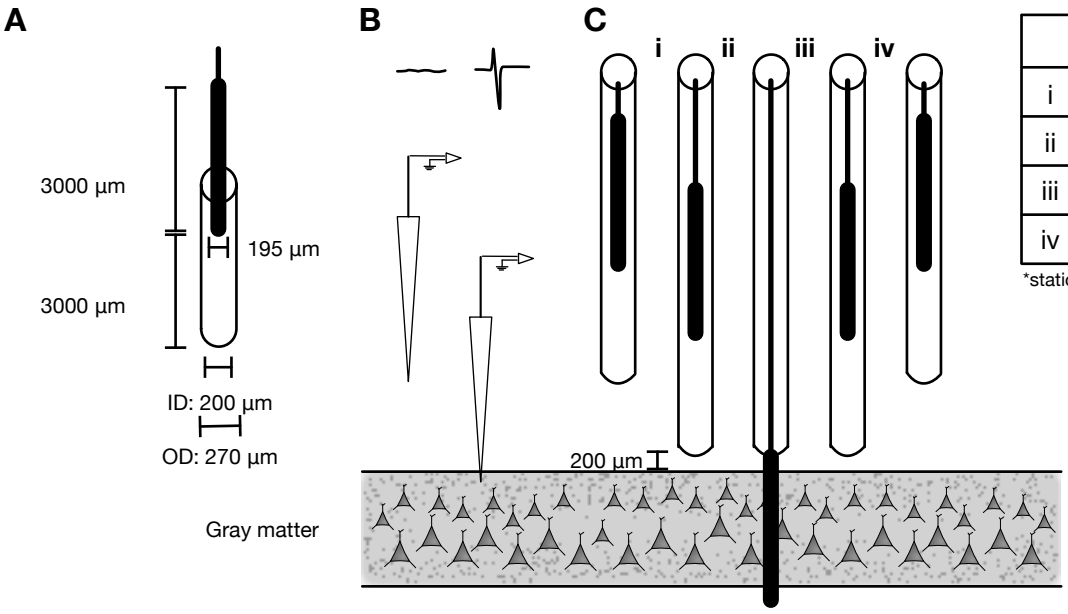

	fibre	cannula	time
i	30 µm/s	30 µm/s	variable
ii	30 µm/s	-	200s
iii	30 µm/s	-	1200s* + 200s
iv	30 µm/s	30 µm/s	variable

*stationary: extraction period of 20 min

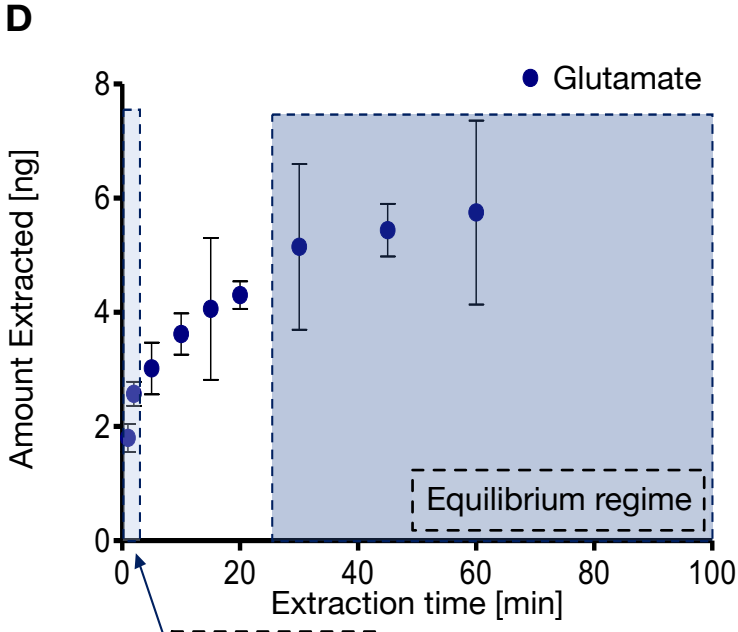

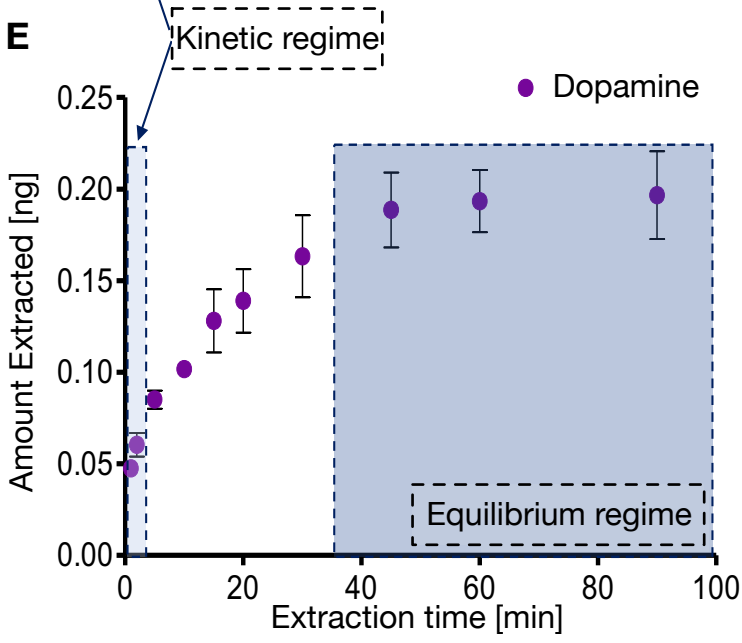

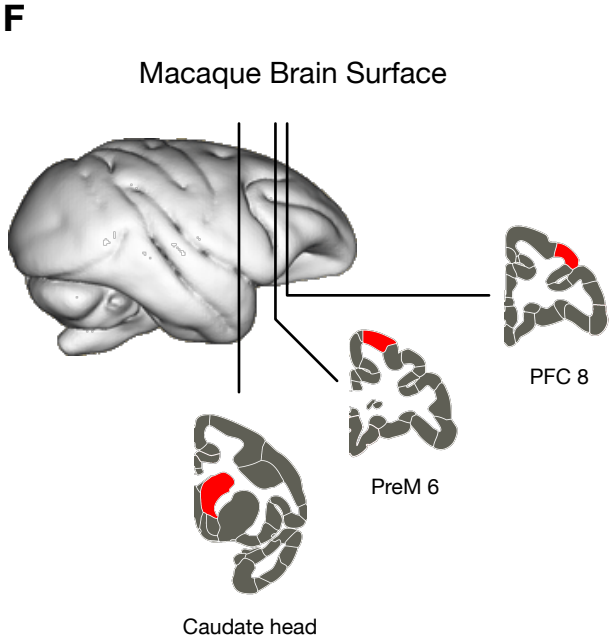

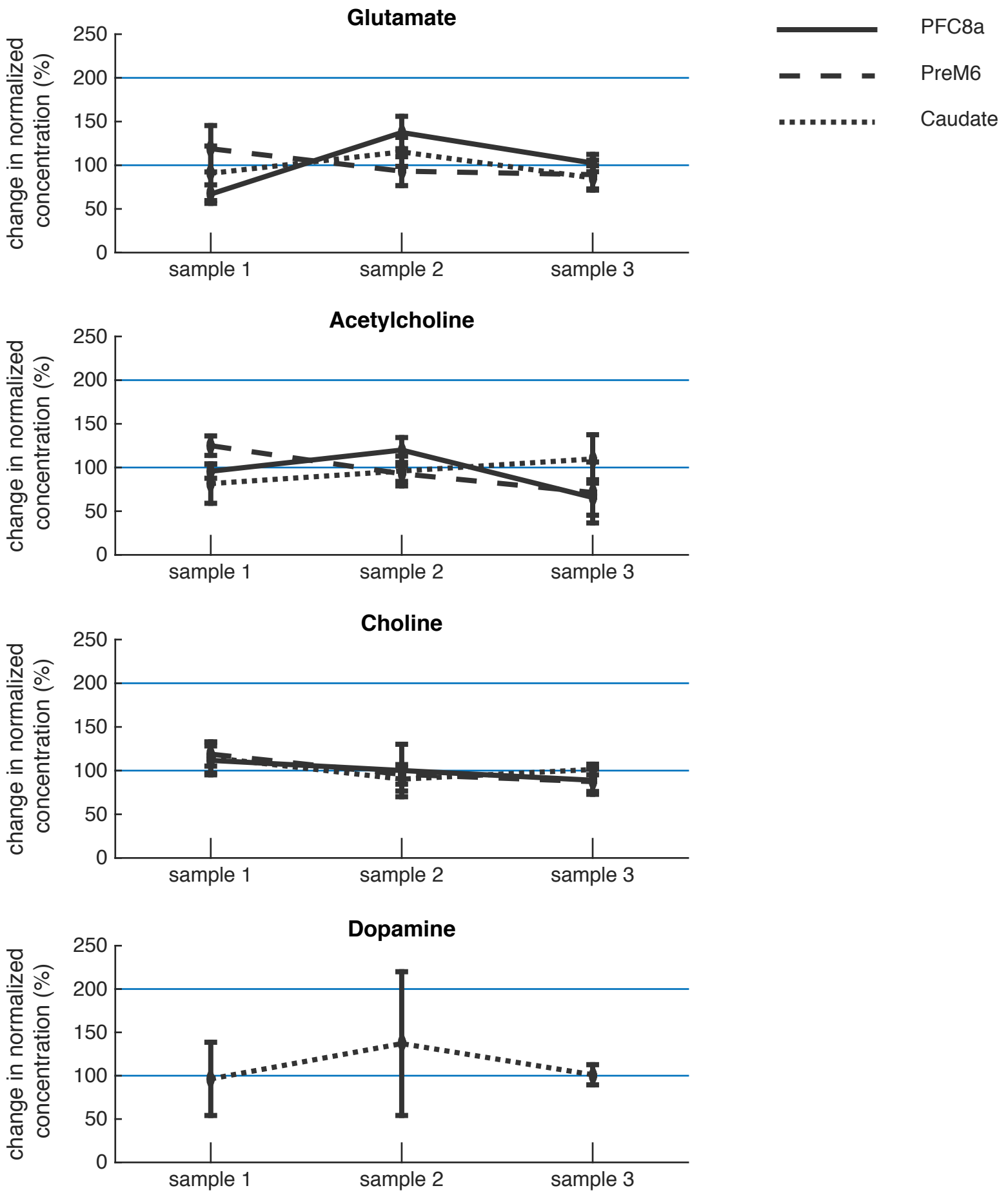
Glutamate
Acetylcholine
Choline
Dopamine
change in normalized concentration (%)
250
200
150
100
50
0
sample 1
sample 2
sample 3
PFC8a
PreM6
Caudate

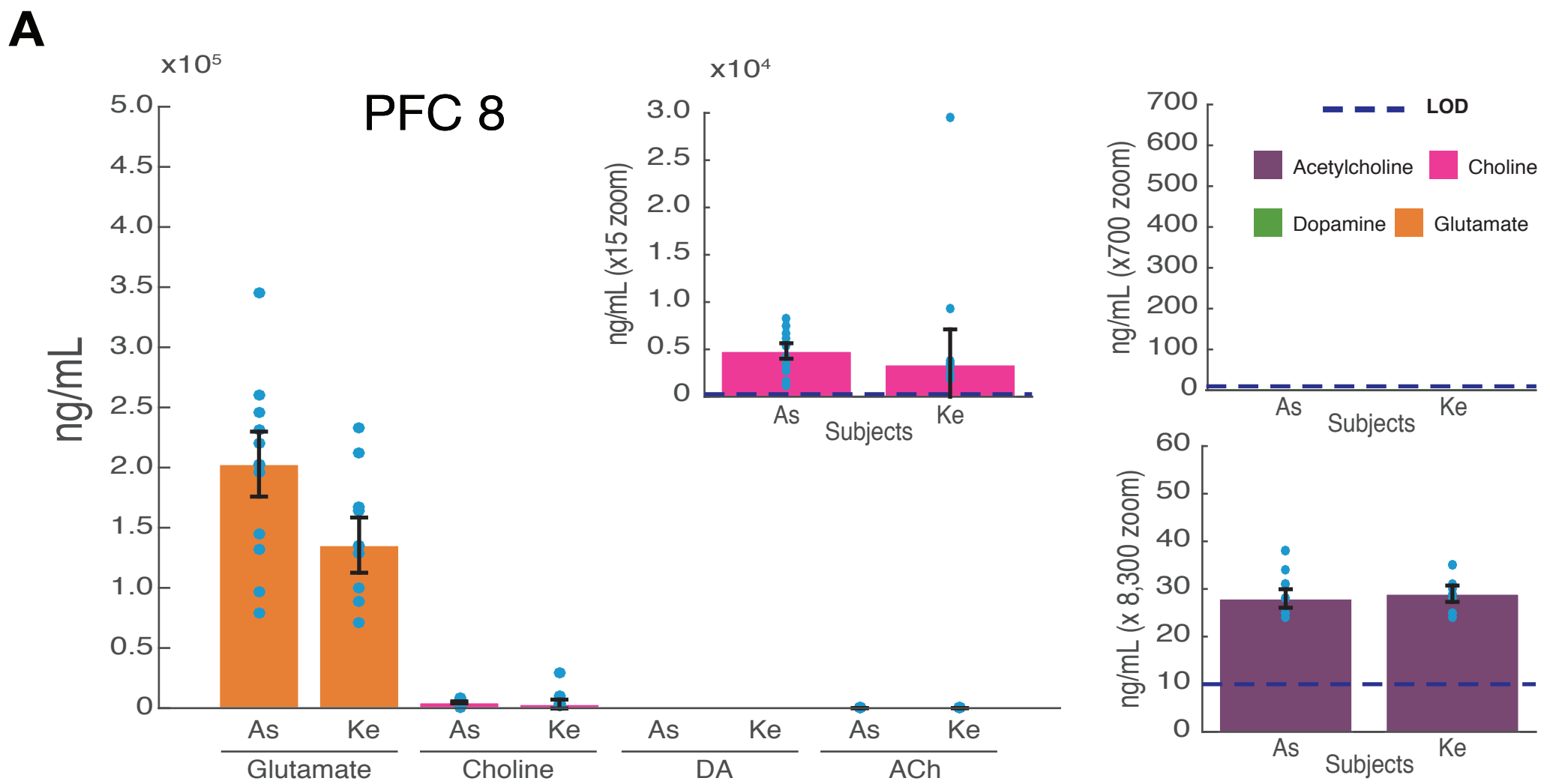
A
PFC 8
x10⁵
ng/mL
5.0
4.5
4.0
3.5
3.0
2.5
2.0
1.5
1.0
0.5
0
As
Ke
Glutamate
Choline
DA
ACh
x10⁴
ng/mL (x15 zoom)
Subjects
LOD
Acetylcholine
Choline
Dopamine
Glutamate
ng/mL (x700 zoom)
ng/mL (x 8,300 zoom)

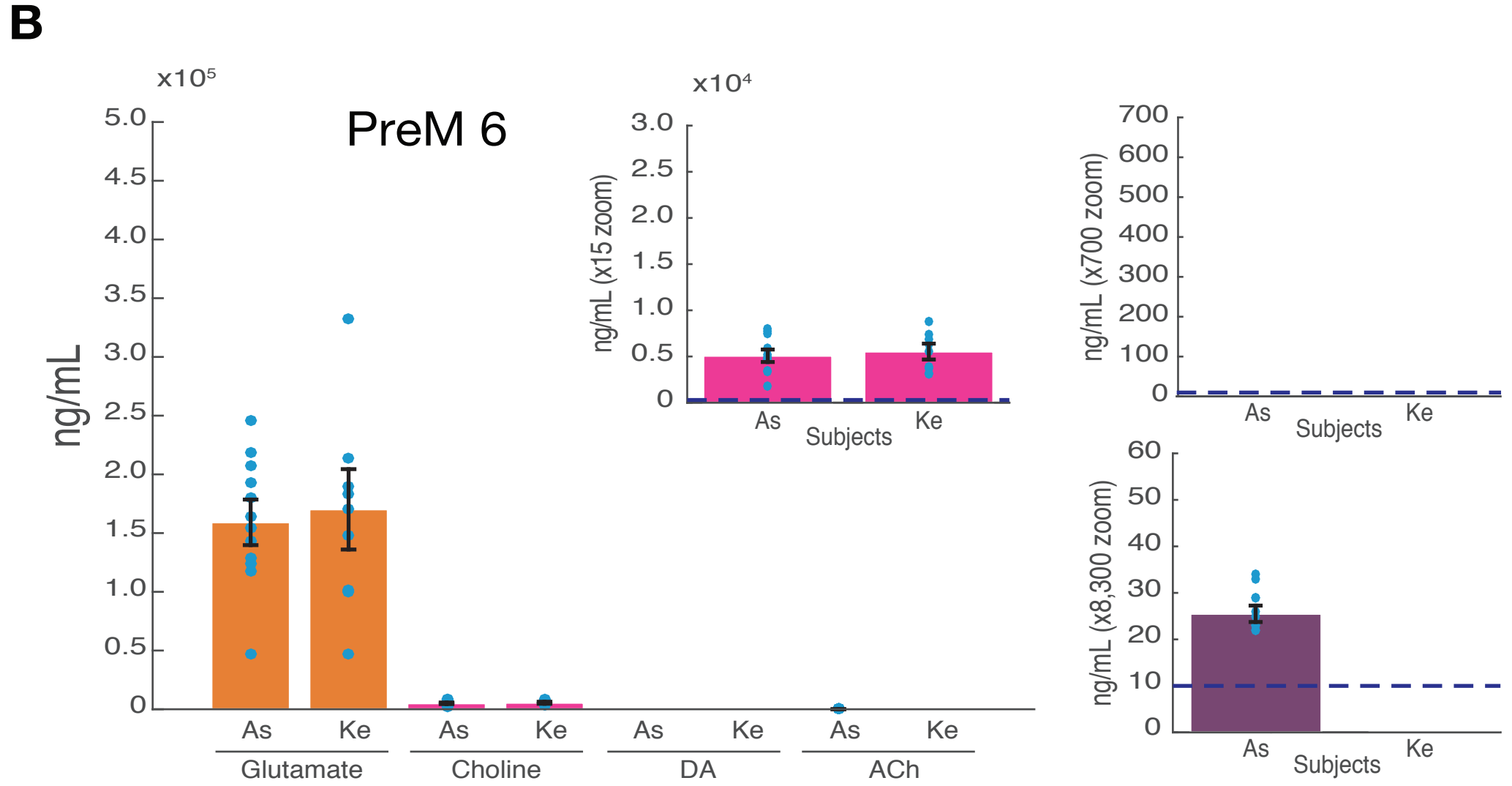
B
PreM 6
x10⁵
ng/mL
5.0
4.5
4.0
3.5
3.0
2.5
2.0
1.5
1.0
0.5
0
As
Ke
Glutamate
Choline
DA
ACh
x10⁴
ng/mL (x15 zoom)
Subjects
ng/mL (x700 zoom)
ng/mL (x8,300 zoom)

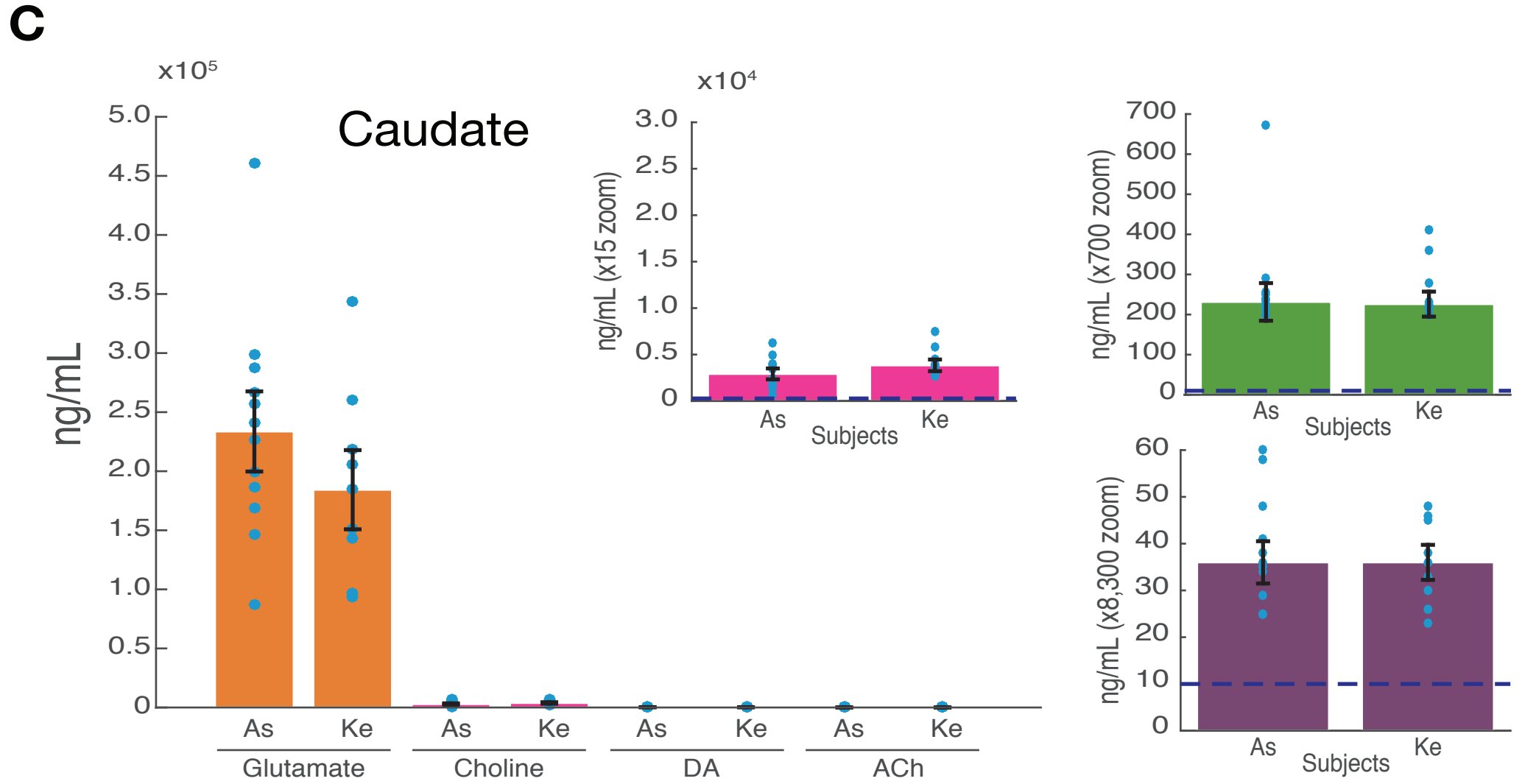
C
Caudate
x10⁵
ng/mL
5.0
4.5
4.0
3.5
3.0
2.5
2.0
1.5
1.0
0.5
0
As
Ke
Glutamate
Choline
DA
ACh
x10⁴
ng/mL (x15 zoom)
Subjects
ng/mL (x700 zoom)
ng/mL (x8,300 zoom)

Supplementary Methods

Chemicals, Reagents and Materials

The LC-MS-grade solvents methanol (MeOH), acetonitrile (ACN), isopropanol (IPA) and water, as well as the acetylcholinesterase inhibitor phenylmethylsulfonyl fluoride (PMSF) were purchased from Fisher Scientifc. Formic acid, polyacrylonitrile (PAN), N,N-dimethylformamide (DMF) and the standards of neurotransmitters: γ-aminobutyric acid (GABA), glutamic acid (Glu), acetylcholine (ACh), histamine (Hist), serotonin (5-HT), dopamine (DA) and choline (Cho) as well as their deuterated analogues were purchased from Millipore Sigma (Oakville, ON, Canada). Epinephrine (Epi), norepinephrine (NE) and their deuterated analogues were obtained from Cerilliant Corporation (Round Rock, TX, USA). Choline-D9, was purchased from Cambridge Isotope Laboratories (Tewksbury, MA, USA). The reagents used for synthesis of hydrophilic-lipophilic balance polymer particles functionalized with strong cation exchange groups, as well as compounds for preparation of PBS were purchased from Millipore-Sigma. The stainless steel wire (stainless steel grade AISI 304, 150 µm diameter) used for manufacturing of SPME probes was purchased from Unimed S.A. (Lausanne, Switzerland). The stainless steel tubing used as guiding cannulas (270 µm O.D.; 200±5 µm I.D.) was obtained from Vita Needle (Needham, MA, USA).

LC-MS/MS Analysis

On the day of analysis, the SPME probes were defrosted and desorbed into 40 µL of water/ACN/MeOH 40:30:30 (v/v/v) mixture containing 1 % of formic acid and a mixture of deuterated isotopologues of targeted neuromodulators (used as internal standards, IS) at 20 ng/mL. The desorption was carried out for 1 h with agitation at 1500 rpm. The extracts were injected into the LC-MS system for targeted neurotransmitter analysis within a few hours after desorption. All experiments were carried out using an Ultimate 3000RS HPLC system coupled to TSQ Quantiva triple quadrupole mass spectrometer (Thermo Fisher Scientific, San Jose, California, USA). Data processing was performed using Thermo software Xcalibur 4.0 and Trace Finder 4.1. For chromatographic separation of the target compounds, a modified method of what is previously reported (Cudjoe and Pawliszyn 2014) was used, adjusted to include more

targeted neuromodulators and their corresponding IS. A Kinetex® PFP LC column (100 x 2.1 mm, 1.7 µm; Phenomenex, Torrance, CA, USA) was held at 30°C with the mobile phase flow rate at 400 µL/min. The mobile phase A consisted of water/MeOH/ACN 90:5:5 (v/v/v) with 0.1 % formic acid, and mobile phase B was ACN/water 90:10 (v/v) with 0.1% of formic acid. The chromatographic gradient was applied starting from 100% B for 1 min and increasing the aqueous mobile phase A to 100% for 3 min with convex gradient function, held for 0.5 min and subsequent linear return to initial conditions and re-equilibration for 1 min, yielding total time of 6.5 min. The injection volume was 10 µL. MS/MS analysis was performed with electrospray ionization in positive mode under selected reaction monitoring conditions, with two MS/MS transitions for each neuromodulator (quantifier and qualifier) and one for each IS.

Quantitation of neuromodulators

Individual stock standard solutions of all targeted neuromodulators were prepared in methanol or water with 0.1% formic acid at a concentration of 1 mg/mL and stored at −80 °C for maximum of one month. In order to calculate the amounts of neuromodulators extracted by each probe, calibrator standards prepared in the same desorption solvent as real samples were analyzed in the same batch. This instrumental calibration curve was prepared in the range of 0.1-200 ng/mL by a serial dilution of the stock standard mixture of all compounds at 1µg/mL. The IS concentration was kept constant at 20 ng/mL in all calibrators, identically as in the real samples. The amounts extracted were calculated based on linear regression equation obtained from the analytical signal (the ratio of chromatographic peak areas of analytes and their corresponding IS) plotted against the concentration.

In order to calculate the concentrations of neuromodulators in brain, matrix-matched external calibration approach was used. The surrogate matrix consisted of 2% agar gel mixed with brain homogenate in the ratio 1:1 (*v/w)*. The homogenized brain tissue was earlier incubated with 1 mM PMSF for 1 h at 37°C to prevent enzymatic digestion of acetylcholine in the calibrator samples. Due to several target compounds being present in brain homogenate at high concentrations (e.g. for glutamate and choline the “blank” brain homogenate matrix doesn’t exist), their quantitation was based on signals of their deuterated isotopologues. The calibrator samples were prepared in the surrogate matrix with concentrations of neuromodulators ranging

from 5 to 3000 µg/mL for the isotopically labelled compounds or from 10 to 2000 ng/mL for the remaining compounds.

The extractions were carried out with SPME probes manufactured and pre-treated identically to the probes used for *in vivo* sampling and using the same 20 min extraction time and desorption conditions as for the real samples. The amounts of neuromodulators extracted from the calibrator samples were determined in the same way as described above and plotted against concentrations of calibrators. The resulting weighted linear regression equations were applied to the amounts of neuromodulators extracted from the *in vivo* samples, yielding values of concentrations of the compounds of interest in brain.

The limits of detection (LOD) were estimated as the levels corresponding to the signal to noise ratio of 3 and were calculated based on the signal of blank calibrator sample (considered as the noise).

Supplementary Results

Observed serotonin concentrations. Overall, serotonin concentrations were not observed as reliably as the other reported neurochemicals and therefore were excluded from the main analyses. However, in one of the animals, serotonin was observed near the LOD in the prefrontal cortex as well as the caudate in a subset of probes. Within the 9 probes placed in both areas, serotonin was detected in 22% of samples (2/9 probes) in the prefrontal cortex and 33% of samples (3/9 probes) in the caudate nucleus. Serotonin observations ranged from 149 ng/mL to 232 ng/mL with a median of 171 ng/mL (±18.5 ng/mL; standard error of the median) with a LOD of 100 ng/mL. The proximity of the measurements to the LOD suggest that the other probes likely collected concentrations of serotonin below the detection threshold. No serotonin observations were made in the second animal.

Supplementary Discussion

Future adjustments to the SPME neurochemical sensing. Several improvements to the protocol can be made in order to make SPME more informative. Using a more sensitive MS would reduce detection thresholds and increase sensitivity in detecting compounds not

successfully measured here such as GABA, serotonin or norepinephrine. This would be very impactful, especially in the case of Serotonin for reasons discussed above. Additionally, efforts could be made to improve the extracting phase synthesis and functionalization protocols and increase the extracting capabilities of SPME probes. Moreover, in order to decrease the MS background and interferences in the range of small molecules, derivatization strategy could be considered.

For GABA, the most promising strategy is post-desorption derivatization by reagent increasing the compound's hydrophobicity resulting in better MS signal such as benzoyl chloride (Wong 2016). Catecholamine and acetylcholine detection may be improved by optimizing the post-sampling analysis pipeline. Improvements can be made at several steps in order to better preserve and quantify catecholamines: (1) faster coupling of sampling to desorption (2) trying various antioxidant solutions and other preservatives for maintaining catecholamine integrity and (3) faster analysis of the desorbed analytes. Faster coupling of sampling to desorption could be achieved through a more stream-lined process of fibre placement and retraction involving a static cannula maintained through several sampling events. This mechanism would also allow for a faster replacement of SPME probes resulting in a shorter delay between consecutive measurements.

A preliminary experiment using spiked artificial cerebra-spinal fluid (aCSF) with very high, known concentrations of all target compounds yielded detectable concentrations of all target compounds indicating that the extracting phase of the SPME probe is capable of capturing all compounds of interest. Furthermore, simultaneously collected replicates displayed very little loss of collected compounds over several days when placed in a -80°C freezer (data not shown). Such findings neither support nor antagonize the suggested strategies for improving SPME yield and sensitivity in primates as detection properties within the aCSF do not seem to accurately reflect those observed in vivo in NHPs. This is likely contributed to by the dynamic and highly regulated nature of target compounds within the extracellular space of the brain and the dynamic equilibrium between the extracting phase of the SPME probes and the extracellular environment. Further tests of the possible differences between these two mediums and improvement strategies to SPME probes are subject for future studies.

Supplementary Figures

Fig S1. Experimental procedure from SPME probe fabrication to quantitation. Fabrication described the in-house procedure to prepare SPME probes. Preparation describes experimental set-up. Sampling describes the actual data collection process. LC/MS analysis describes the chemical quantitation of collected data samples.

Supplementary Tables

Table 1. Overview of in vivo neurochemical measurement methods

	PET imaging	**Electro-chemistry**	**Micro-dialysis**	**Solid phase micro-extraction**
Temporal Resolution	Minutes	Highest (millisecond range)	1-30 minutes (usually 20 minutes); dependent on MS sensitivity, target etc.	<5-30 minutes; dependent on MS sensitivity, coating thickness, target etc.
Spatial Resolution	Voxel	High; surface area may vary (relevant for enzyme based methods)	Diffusion based; surface area may vary	Diffusion based; surface area may vary
Sensitivity	Indirect measurement via competitive radiolabeled species	High	Depending on post-hoc methods (i.e. MS)	Depending on post-hoc methods (i.e. MS)
Neuro-active targets	A few at most	A few at most	Many	Many
Non-neuro-active targets	No	No	Yes, greater efficacy for hydrophilic compounds	Yes, greater potential efficacy for hydrophobic compounds
In vivo feasibility	Difficult in awake, behaving animal models; movement highly restricted	Good (low reliability in NHPs)	Good	Best
Cost	High	Requires special equipment	Requires special equipment	Easy to port to an acute micro-electrode setup; requires a chemistry core

Table S1. A comparison of methods capable of measuring single or multiple neurochemicals in vivo. Temporal resolution, spatial resolution, sensitivity, capability to measure neuro-active and non-neuro-active compounds, in vivo feasibility and cost. PET: positron emission tomography; NHP: non-human primate; MS: mass spectrometer.

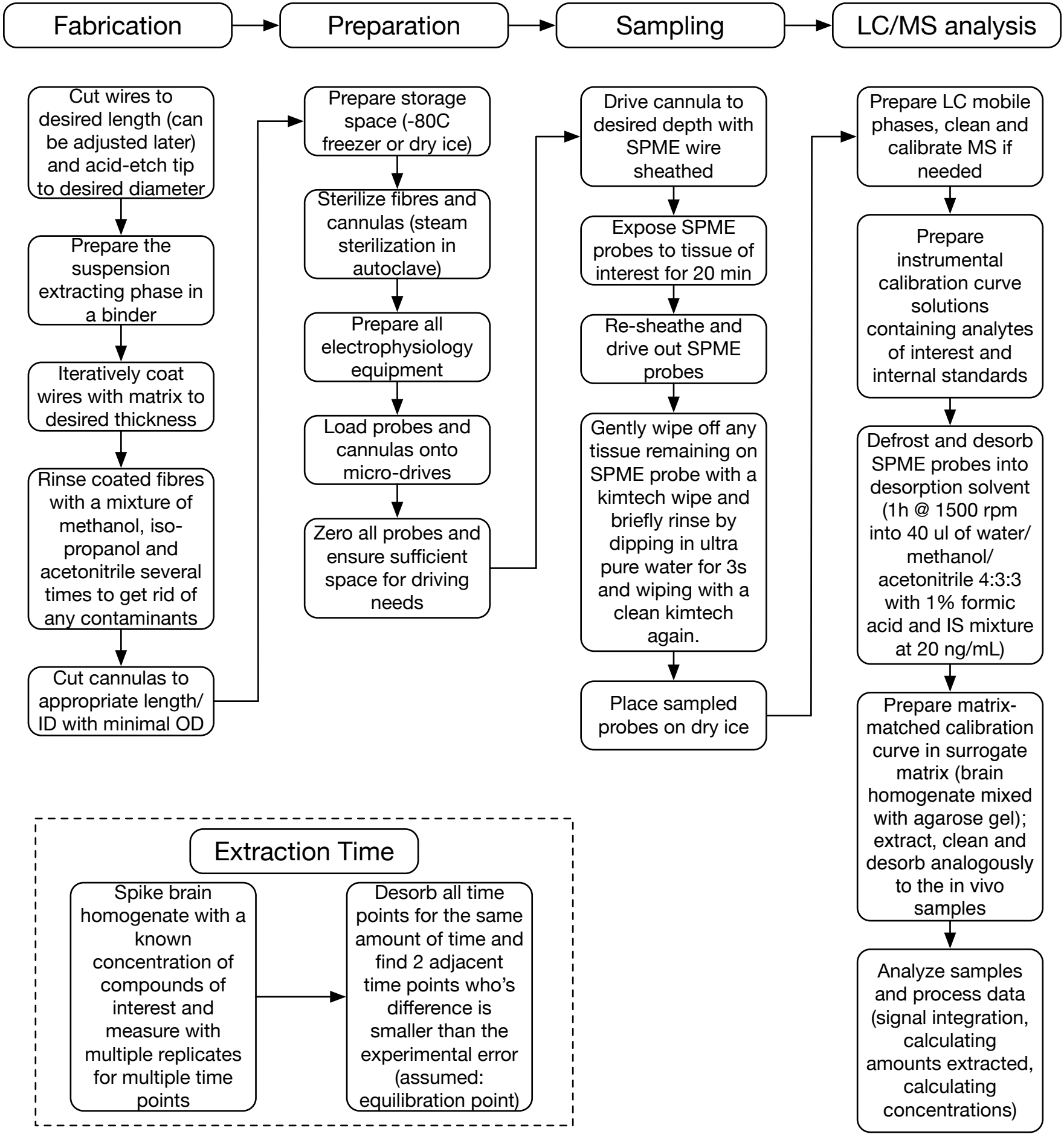
Fabrication
Preparation
Sampling
LC/MS analysis
Cut wires to desired length (can be adjusted later) and acid-etch tip to desired diameter
Prepare the suspension extracting phase in a binder
Iteratively coat wires with matrix to desired thickness
Rinse coated fibres with a mixture of methanol, iso-propanol and acetonitrile several times to get rid of any contaminants
Cut cannulas to appropriate length/ ID with minimal OD
Prepare storage space (-80C freezer or dry ice)
Sterilize fibres and cannulas (steam sterilization in autoclave)
Prepare all electrophysiology equipment
Load probes and cannulas onto micro-drives
Zero all probes and ensure sufficient space for driving needs
Drive cannula to desired depth with SPME wire sheathed
Expose SPME probes to tissue of interest for 20 min
Re-sheathe and drive out SPME probes
Gently wipe off any tissue remaining on SPME probe with a kimtech wipe and briefly rinse by dipping in ultra pure water for 3s and wiping with a clean kimtech again.
Place sampled probes on dry ice
Prepare LC mobile phases, clean and calibrate MS if needed
Prepare instrumental calibration curve solutions containing analytes of interest and internal standards
Defrost and desorb SPME probes into desorption solvent (1h @ 1500 rpm into 40 ul of water/ methanol/ acetonitrile 4:3:3 with 1% formic acid and IS mixture at 20 ng/mL)
Prepare matrix-matched calibration curve in surrogate matrix (brain homogenate mixed with agarose gel); extract, clean and desorb analogously to the in vivo samples
Analyze samples and process data (signal integration, calculating amounts extracted, calculating concentrations)
Extraction Time
Spike brain homogenate with a known concentration of compounds of interest and measure with multiple replicates for multiple time points
Desorb all time points for the same amount of time and find 2 adjacent time points who's difference is smaller than the experimental error (assumed: equilibration point)